Article

Mach Number Prediction for 0.6 m and 2.4 m Continuous Transonic Wind Tunnels

Luping Zhao *[ID]**, Wei Jia and Yawen Shao**

College of Information Science and Engineering, Northeastern University, Shenyang 110819, China;
jiawei__1120@163.com (W.J.); sywdream7@163.com (Y.S.)
* Correspondence: zhaolp@ise.neu.edu.cn; Tel.: +86-188-4255-2385

Abstract: With the development of the design technology, more and more advanced and diverse wind tunnels have been constructed to match complex requirements. However, it is hard to design a precise physical model of a wind tunnel that can be controlled. In addition, if a new wind tunnel is designed, the experimental data may be insufficient to build a controlling model. This article reports research on the following two models: (1) for a 0.6 m continuous transonic wind tunnel supported by a large amount of historical data, the false nearest neighbor (FNN) algorithm was adopted to calculate the order of the input variables, and the nonlinear auto-regressive model with the exogenous inputs–backpropagation network (NARX-BP) was proposed to build its Mach number prediction model; (2) for a new 2.4 m continuous transonic wind tunnel with only a small amount of experimental data, the method of model migration, the input and output slope/bias correction–particle swarm optimization (IOSBC-PSO) algorithm, was developed to convert the old model of the 0.6 m wind tunnel into the new model of the 2.4 m wind tunnel, so that the new Mach number prediction could be conducted. Through simulation experiments, it was found that by introducing the NARX-BP algorithm to build the Mach number prediction model, the root-mean-square error (RMSE) of the model decreased by 44.93–77.90%, and the maximum deviation (MD) decreased by 64.05–85.32% compared to the BP model. The performance of the IOSBC-PSO migration model was also better than that of the non-migration model, as evidenced by the 82.06% decrease of the RMSE value and the 78.25% decrease of the MD value. The experiments showed the effectiveness of the proposed strategy.

Keywords: continuous transonic wind tunnel; prediction model; model migration; FNN algorithm; NARX-BP algorithm; IOSBC-PSO algorithm

1. Introduction

To study aerodynamics and design aircrafts, wind tunnels, especially the continuous transonic wind tunnel (CTWT), have become indispensable. Over the past two decades, the research and practical application of wind tunnels have received increasing attention, as they are widely applied in many fields based on aerodynamic theories [1,2] and in the design of many artifact including bridges [3], buildings [4], trains [5] and aircrafts [6–8]. It should be especially noted that wind tunnel experimentation has great significance for wind farm research, as it can help to model the inter-farm cluster interaction of the wind power base [9]. The latter is of great value when studying the impact of wind farms on the local and regional atmospheric boundary layer [10]. Research on wind tunnels is rich and detailed [11–15]. Since a large number of wind tunnels appeared in the middle of the 20th century, the design and use of wind tunnels are always improving.

Wind tunnel control has always been an important research topic. Control accuracy, adjustment speed and stability of the Mach number of the wind tunnel flow field are the key factors to measure the performance of a wind tunnel system. The traditional wind tunnel control method is based on the PID controller [16–18], but with the design of wind tunnels becoming more sophisticated, higher requirements such as nonlinearity and robustness

have emerged. The PID control can no longer satisfy the demands. As a result, some intelligent algorithms for wind tunnel control are being studied. In addition, there are other problems such as the modeling complexity, the inaccuracy of the Mach number measurement and the difficulties to obtain process variables.

The Mach number is an important evaluation index of the wind tunnel system. The essence of wind tunnel control is to stabilize the air velocity in the wind tunnel, i.e., the Mach number, at a set value. There are many factors affecting the stability of the Mach number, and the wind tunnel model is supposed to be as precise as possible. Moreover, the characteristics of wind tunnel systems are not the same, and the modeling methods are naturally different. Even for the same wind tunnel, different uses or different working conditions will lead to differences in the wind tunnel system, which makes the modeling process extremely difficult. Thus, it is hard to create an accurate mechanistic model for every wind tunnel. The more direct way is through data processing and mining. A large number of experimental results have revealed the operating mechanism of wind tunnels, which involves process variables such as engine speed, total pressure, static pressure, angle of attack, etc.

Model migration has also been intensively researched by scientists. Model migration aims to build and develop a new model of a process based on an established model, while using less experimental data. Considering the multiple operation modes in the industry, for different working modes, the data-based process modeling must be repeated, and a large number of experiments must be repeated to develop new prediction models. Obviously, this is inefficient and uneconomical. Therefore, in recent years, research on model migration methods has increased. Lu J.D. and other scholars [19] considered the process attribute variables related to the output in the process of studying the migration of family-similar models and considered both the input and output of the old process and the paired attribute variables of the new and old process as the input to build the new process model. Tang [20] used model migration to compress and reconstruct the voltage data of lithium-ion batteries. The above research showed that it is difficult to ensure the accuracy of feature classification in industrial processes with incomplete data. Therefore, a model migration method with low requirements for data features and a simple structure is needed. The Input and Output Slope/Bias Correction (IOSBC) method has emerged [21,22], which utilizes known data under similar operating conditions to migrate models established under historical working conditions. This algorithm requires a small number of samples and low computational complexity, which makes it suitable for model migration in multiple working modes.

Using the known data under similar working conditions, the model migration algorithm, allowing the migration from a model established under historical working conditions to a new model under new working conditions, has been proved effective in a large number of practices; however, not many studies have focused on wind tunnel modeling via model migration.

Based on the above considerations, this study first aimed to obtain a prediction model for a 0.6 m CTWT, which was successfully applied leading to a large amount of experimental data. Once the model was obtained, we aimed to obtain a migration model to describe a 2.4 m CTWT with few experimental data. The primary advantages of our model over previous ones are described below.

(1) Unlike [17,18], the method proposed in this article is a wind tunnel control model based on intelligent algorithms. In comparison to [16], the application of intelligent algorithms is innovative, as they are not simply used to change the PID parameters.

(2) Unlike [12], the wind tunnel modeling method described in this article is not based on a theoretical sophisticated design of wind tunnels, but on experimental results obtained in various working conditions through data analysis and mining. This method is more concise and effective, and due to the complexity of wind tunnel functioning, the input/output-oriented method proposed in this paper may have more practical value.

(3) The model migration algorithm proposed in the paper combines old models and data obtained in new working conditions to migrate the model. The data of the new and old models have their respective roles, rather than being simply combined as the input data of the new model, which is not the case for [19]. Furthermore, the parameters for model migration are provided by intelligent algorithms, which is clearly more scientific than introducing all the factors into a neural network [19,20].

The main contribution of this study is the creatin of a description model for both a 0.6 m CTWT and a 2.4 m CTWT, considering that for the 2.4 m CTWT, there are few experimental data that could be utilized to model it directly. The purpose of the algorithm proposed in this paper is to accurately predict the Mach number in the stable stage of the wind tunnel operation. Therefore, a method is proposed in this paper that combines multiple intelligent algorithms for this purpose, and finally wind tunnel modeling is achieved. The study reported in in this paper is a first approach to wind tunnel control, that is, it presents a set of methodologies and builds a framework for obtaining wind tunnel description models. With the rapid development of intelligent algorithms, our methodology may be improved to obtain more accurate models, which is also a direction of future research.

The rest of this article is as follows.

In Section 2, the prediction model of a 0.6 m CTWT is established, using the FNN approach to determine the order of the input variables and the NARX-BP approach to fit the curve. In Section 3, the IOSBC approach is chosen for model migration for a 2.4 m CTWT, and the PSO algorithm is used to optimize the parameters of the IOSBC model. Finally, the work reported in this paper is summarized in Section 4, and future research directions are suggested.

2. Methodology

2.1. Modeling Methodology for the 0.6 m CTWT

In this subsection, the methodology we used to model the 0.6 m CTWT is described in four steps:

1. Determining the output variables and input variables.
2. Determining the order of the input variables.
3. Building the model using a suitable algorithm.
4. Evaluating the model.

These steps are detailed below.

1. Determining the output variables and input variables

As introduced before, the goal of wind tunnel control is to make the Mach number stable. In the majority of cases, researchers set the Mach number as the output variable of the model, which can intuitively display the fitting degree of the model. Moreover, changes of the input variables could influence the Mach number, and this can be directly observed, which is beneficial for predictive control and can be achieved using the here established prediction model.

The working condition of a CTWT is affected by multiple indicators. Alterations of these variables could directly influence the output of the CTWT model.

According to the analysis of the aerodynamic structure and process flow of the concerned CTWT, the main control variable of this wind tunnel is the actual compressor speed (Sp). There is an interference quantity, namely, the total pressure in the stable section (Ps). The main controlled variable of the flow field system is the Mach number in the test section (Ma), which is mainly affected by the total pressure in the stable section (Ps) and the static pressure in the test section (Pt). These variables are defined below.

(1) Mach number (Ma)

The Mach number is the ratio of the speed of an object to the speed of sound, which is a multiple of the sound velocity, and is a dimensionless number. The Mach number is the

controlled variable in this study, and the previous state of the Mach number has a strong correlation with the Mach number in the current state.

The Mach number studied in this project mainly operated in the transonic range.

(2)   Total pressure (Ps)

The total pressure is the pressure assumed to exist when a gas is stationary in isentropic adiabatic motion and is mainly determined by gas density, temperature, gas constant and pressure. It is measured and recorded in the stable section of a wind tunnel system.

Although the total pressure can be independently debugged and operated in a continuous wind tunnel, there is also a serious coupling phenomenon between the total pressure and the Mach number. During the process of controlling the Mach number with the compressor speed, the total pressure is also constantly changing.

(3)   Static pressure (Pt)

The static pressure is the normal force of the interaction between the flow layers inside a gas, measured and recorded in the test section of a wind tunnel. Static pressure and total pressure jointly determine the magnitude of the Mach number in a wind tunnel system. In the condition that the total pressure is not artificially changed, the static pressure is an important variable that affects the magnitude of the Mach number.

(4)   Compressor speed (Sp)

The compressor speed directly controls the stability of the Mach number, and continuous wind tunnels mainly stabilize the Mach number within the control accuracy range by adjusting the speed.

According to the above description, the total pressure (Pt), static pressure (Ps), compressor speed (Sp) and Mach number (Ma) were chosen as the input variables of this model.

2.   Determining the orders of the input variables

The order of the variables selected for a model will directly affect the accuracy of prediction. A selected low order can lead to incomplete data information and the inability to accurately predict the Mach number, while a selected excessively high order will lead to information redundancy, which will cause too much noise in the model and prevent achieving a fast control. Therefore, the order of the variables should be determined scientifically through algorithms. The commonly used methods to determine the order of variables include the correlation integral (CI) approach [23], the singular value decomposition (SVD) approach [24] and the false nearest neighbor (FNN) approach [25]. The CI approach needs a large sample size and can be easily influenced by noise. The SVD approach is suitable for linear systems but not for nonlinear systems. The FNN approach measures the ability of original features to interpret category variables. Based on the above considerations, the FNN approach was chosen to determine the order of the variables.

As shown in Figure 1, when the dimension is 1, points A, B and C seem to be neighbors as a consequence of projecting into a space of smaller dimensions. However, when the dimension reaches 2, point B becomes separated from A and C. The idea of the FNN algorithm is that neighboring points that are squeezed together by low dimensions cease to be neighboring points as the dimensions increase. The FNN algorithm defines these points as false nearest neighbors. For a time series, when all false nearest neighbors disappear, the determined dimension can lead to information that is neither redundant nor deficient, and this dimension is the best dimension.

The details of the FNN algorithm are as follows.

For the sample data that are known as

$$x_k = [y(k-1), \ldots, y(k-n), u(k-1), \ldots, u(k-n)]^{\mathrm{T}} \tag{1}$$

the calculation of the FNN algorithm can be achieved by the following two methods:
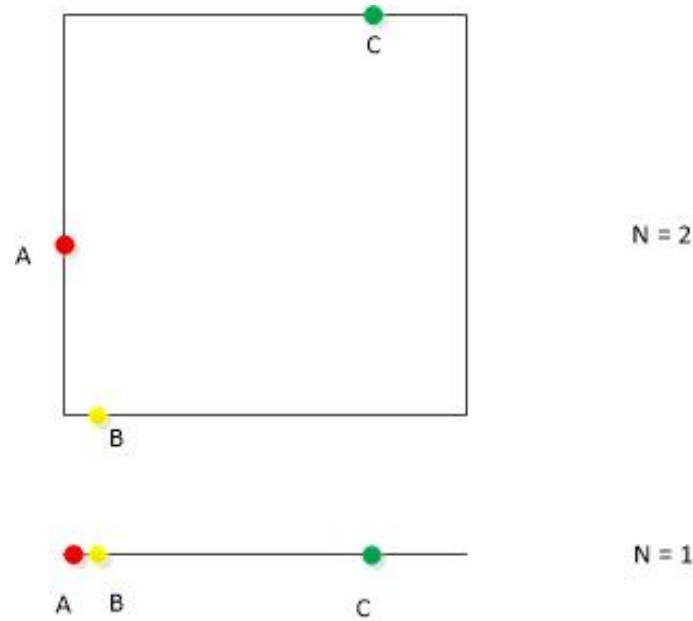
Figure 1. Diagram of false nearest neighbors.

(1) Find the nearest neighbor x_j^n in N-dimensional space to make d_n minimum:

$$d_n = \left\| x_k^n - x_j^n \right\|_2 \tag{2}$$

Judge if the following description is true:

$$\frac{\left| y_k - y_j \right|}{\left\| x_k^n - x_j^n \right\|_2} \le R \tag{3}$$

where R is defined as the critical value, set between 10 and 50, generally 10. If the above formula is false, then the point is a false nearest neighbor.

(2) Increase the dimensions of x_k^n and x_j^n by 1 and calculate d_{n+1}:

$$d_{n+1} = \left\| x_k^{n+1} - x_j^{n+1} \right\|_2 \tag{4}$$

Judge if the following description is true:

$$\frac{d_{n+1}}{d_n} \le R \tag{5}$$

where R is defined as the critical value, set between 10 and 50, generally 10. If the above formula is false, then the point is a false nearest neighbor.

As long as one of the above two judgements is false, the point can be considered as a false nearest neighbor. Judge every moment k, calculate the percentage of all moments with pseudo-neighbor points, change the value of n and continue to judge until the inflection point of the percentage decline is found. At this time, n is the best variable order.

3. Building the model using a suitable algorithm

Considering the time delay of the system, both current and previous states of the above variables are supposed to be input variables. For the modeling of time series, the NARX model [26,27] is most commonly used in the industry. It has the characteristics of memory feedback, can increase the dynamic learning ability and can keep the system output delay and feedback to the input.

The basic structure of the NARX model is as follows:

$$\widetilde{y}(t) = f(y(t-1), \ldots, y(t-n_y), x_1(t-1), \ldots, x_1(t-n_x), \ldots, x_i(t-1), \ldots, x_i(t-n_x)) \quad (6)$$

where $y(t-1), \ldots, y(t-n_y)$ express the historical output sequence of the model, $x_i(t-1), \ldots, x_i(t-n_x)$ express the historical input sequence of the model, i is the type number of the input variables, and f is the fitting function of the NARX model.

In the selection of the fitting function, the BP network [28] stands out with its strong nonlinear mapping ability, good fault tolerance ability and strong adaptive ability and becomes the best option for the nonlinear fitting function.

According to the above descriptions, a 0.6 m CTWT modeling method was obtained. The previous states of *Pt*, *Ps*, *Sp* and *Ma* were selected as input variables, aiming to predict the Mach number at the next moment. The FNN algorithm was used to determine their orders. Once the order was determined, the data was introduced into the NARX-BP-based prediction model to obtain the prediction result.

4.   Evaluating the model

When a model is established, evaluation indicators are supposed to be utilized. Generally, the RMSE is selected to evaluate the prediction of the Mach number. The RMSE measures the deviation between the predicted value and the real value as shown below:

$$RMSE = \sqrt{\frac{1}{N} \sum_{n=1}^{N} \left(Ma(n) - \widetilde{Ma}(n) \right)^2} \quad (7)$$

where $Ma(n)$ is the real wind tunnel output, $\widetilde{Ma}(n)$ is the model predicted value, and n is the number of sampling points. The smaller the RMSE value is, the more accurate the prediction of the model is.

Moreover, the MD is introduced to estimate the maximum prediction deviation between the actual value and the predicted value in the whole prediction process. It can be calculated by

$$MD = \max \left| Ma(n) - \widetilde{Ma}(n) \right| \quad (8)$$

If the MD is too large, the control method will need further improvement.

These two evaluation indicators have different significance. A low RMSE indicates high stability and accuracy of prediction, while the MD represents the maximum error that the system can support. The project requires an RMSE of less than 0.001 of and an MD of less than 0.001.

In conclusion, the establishment process of the FNN-NARX-BP Mach number prediction model for a single working condition is shown in Figure 2.

2.2. Modeling Methodology for the 2.4 m CTWT

The previous section discussed a set of modeling methods for a 0.6 m CTWT. However, the FNN-NARX-BP method is based on the assumption that a large amount of experimental data can be used to build the prediction model. Usually, very few data are available to establish a precise prediction model for a new process. Moreover, though some working conditions are similar, directly using a former condition's model to predict the Mach number of the new condition will lead to some prediction errors. In other cases, a new wind tunnel has just been built, whose physical characteristics are similar to those of a wind tunnel with an established prediction model. In view of the fact that a single wind tunnel experiment requires a large amount of money and resources, it is uneconomical and unnecessary to rebuild an all-new prediction model in the above cases. To meet the modeling requirements, a new approach is proposed in this paper, which aims to utilize both the established model of the 0.6 m CTWT and few experimental data of the 2.4 m CTWT to build a description model of the 2.4 m CTWT.
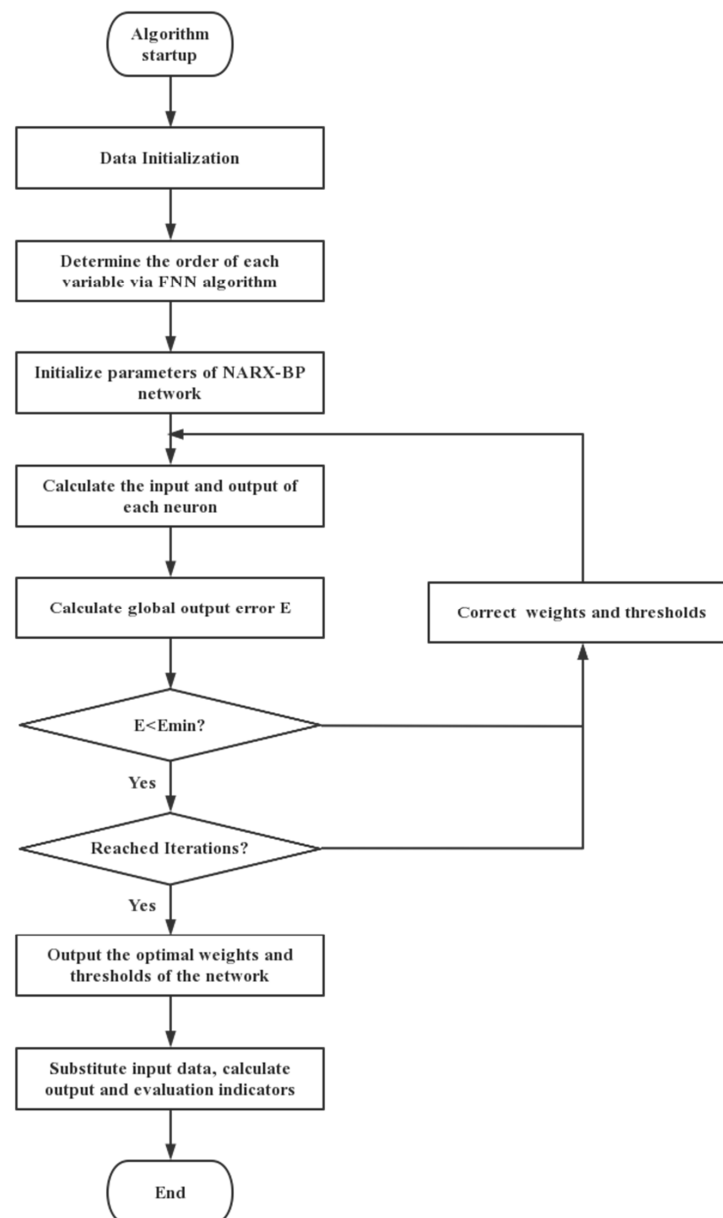
Figure 2. Flow chart of the Mach number FNN-NARX-BP model design.

In this subsection, the methodology used to model the 2.4 m CTWT is described in three steps:

1. Determining the migration algorithms.
2. Determining the intelligence algorithms to obtain the best migration coefficients.
3. Identifying the parameters that will be migrated.

These steps are detailed below.

1. Determining the migration algorithms

How to use a small amount of new working condition data to correct the basic model and obtain a new model is a problem worth solving. Many studies have been conducted on this topic. Section 1 introduced some model migration algorithms. Among these algorithms, the IOSBC model based on the shift and scaling of the historical process proposed by Gao F.R. and Lu J.D. [21] and used in certain applications [22] attracted the attention of the authors. This method is widely used in model migration due to its advantages of simple structure, requirement of less samples and easy combination with other algorithms.

The basic implementation steps of the IOSBC algorithm are as follows.

In the simplest case, a new process is a shift and scaling of an old process. The previous model for any form is as follows:

$$Y_{base} = f(X_{base}) \tag{9}$$

where X_{base} and Y_{base} are the inputs and outputs of the basic model, respectively, and f is any nonlinear function to describe the old process. If there exists a shift and scaling in the input and output space, X_{new} and Y_{new} should be transformed into those of the old process, X_{base} and Y_{base}, by a slope and bias correction:

$$\begin{cases} X_{new} = S_I X_{base} + B_I \\ Y_{new} = S_O Y_{base} + B_O \end{cases} \tag{10}$$

where S_I and B_I denote the scaling and shift of the old process in the input space, and S_O and B_O denote the scaling and shift of the old process in the output space. Thus, the new model is described by the new equation below:

$$Y_{new} = S_O f(S_I X_{base} + B_I) + B_O \tag{11}$$

Through the optimization algorithm, a small amount of known data under the new working condition are introduces, and the following equations are optimized to obtain the optimization parameters:

$$\begin{cases} \text{argmin} J(S_I, B_I, S_O, B_O) = \varepsilon \varepsilon^T \\ \varepsilon = Y - Y_2 \end{cases} \tag{12}$$

2. Determining the intelligence algorithms to obtain the best migration coefficients

As a global optimization algorithm among intelligent optimization algorithms, particle swarm optimization (PSO) can iteratively optimize the parameters of the IOBSC algorithm to find the optimal solution; so, the IOSBC-PSO algorithm was developed in this paper to achieve a better migration of the basic model according to a small amount of data under the new working conditions.

Particle Swarm Optimization (PSO) is a metaheuristic optimization technique inspired by the social behavior of bird flocking or fish schooling. It was first introduced by Kennedy and Eberhart in 1995 [29].

In PSO, a set of particles moves around in a search space to find the optimal solution. Each particle represents a potential solution to the problem being solved. The position of each particle is influenced by its own best-known position as well as by the best-known position among all particles in the swarm. The velocity of each particle is also updated using these two positions.

The algorithm works iteratively, with each iteration consisting of updating the positions and velocities of all particles in the swarm. This process continues until a stopping criterion is met, such as reaching a maximum number of iterations or achieving a desired level of fitness.

PSO has been used to solve a wide range of optimization problems, including function optimization, feature selection, clustering and neural network training. It is known for its simplicity, fast convergence, and ability to find good solutions in high-dimensional search spaces.

The general steps of the PSO algorithm are as follows [28–30]:

1. Initialize a swarm of particles with random positions and velocities in the search space.
2. For each particle, evaluate its fitness value based on its current position.
3. Update the particle's best-known position (*pbest*) if its current fitness value is better than its previous *pbest*.
4. Determine the global best-known position (*gbest*) among all particles in the swarm.

5. Update the velocity and position of each particle using the following equations:

$$\begin{cases} v_i^d = w \cdot v_i^{d-1} + c_1 \cdot rand \cdot r_1 (pbest_i^d - x_i^d) \\ \quad + c_2 \cdot rand \cdot r_2 (gbest^d - x_i^d) \\ \quad\quad x_i^{d+1} = x_i^d + v_i^d \end{cases} \tag{13}$$

where v_i^d is the speed of the particle i at time d, w is the inertia weight, c_1 is the cognitive component, c_2 is the social component, $pbest_i^d$ and $gbest^d$ are the optimal locations of individuals or the whole population, and x_i^d is the position of the particle i at time d.

The inertia weight w controls the impact of the particle's current velocity, the cognitive component c_1 controls the particle's memory of its own best-known position, and the social component c_2 controls the particle's interaction with the swarm.

6. Repeat steps 2–5 until a stopping criterion is met (e.g., maximum number of iterations or desired level of fitness).

The search of each bird in PSO is directional, while the mutation in the genetic algorithm (GA) is random. To some extent, PSO is more efficient than the GA. Moreover, the calculation required by the GA is far greater than that of PSO. In terms of computing effect, PSO is better at dealing with the continuous changes of the variables than the GA [31].

3. Identifying the parameters that will be migrated

Here, we describe the process of model migration of the NARX-BP model established using the IOSBC-PSO method:

The structure of the model is:

$$Ma_p(k) = f_o(\mathbf{W}_h(f_i(\mathbf{W}_i r(k) - \mathbf{B}_i)) - \mathbf{B}_h) \tag{14}$$

where

$$\mathbf{W}_i = \begin{bmatrix} w_{11} & \cdots & w_{1n} \\ \vdots & \ddots & \vdots \\ w_{l1} & \cdots & w_{ln} \end{bmatrix} \mathbf{B}_i = \begin{bmatrix} b_1 & \cdots & b_l \end{bmatrix}^{\mathrm{T}}$$

$$\mathbf{W}_h = \begin{bmatrix} w'_{11} & \cdots & w'_{l1} \\ \vdots & \ddots & \vdots \\ w'_{q1} & \cdots & w'_{ql} \end{bmatrix}, \mathbf{B}_h = \begin{bmatrix} b'_1 & \cdots & b'_q \end{bmatrix}^{\mathrm{T}} \tag{15}$$

where $Ma_p(k)$ is the Mach number normalized, $\mathbf{W}_i$ is the link weight matrix between the input layer and the hidden layer, $\mathbf{B}_i$ is the threshold matrix of each neuron in the hidden layer, $\mathbf{W}_h$ is the link weight matrix between the hidden layer and the output layer, and $\mathbf{B}_h$ is the threshold matrix of each neuron in the output layer. f_m is the activation function between the input layer and the middle layer, and f_o is the activation function between the middle layer and the output layer.

The IOSBC algorithm is used for parameter migration of the optimal weight of each threshold matrix mentioned above. The matrix after the migration is as follows:

$$\mathbf{W}_{im} = \begin{bmatrix} s_{11} \times w_{11} + m_{11} & \cdots & s_{1n} \times w_{1n} + m_{1n} \\ \vdots & \ddots & \vdots \\ s_{l1} \times w_{l1} + m_{l1} & \cdots & s_{ln} \times w_{ln} + m_{ln} \end{bmatrix} \mathbf{B}_{im} = \begin{bmatrix} s_1 \times b_1 + m_1 & \cdots & s_l \times b_l + m_l \end{bmatrix}^{\mathrm{T}}$$

$$\mathbf{W}_{hm} = \begin{bmatrix} s'_{11} \times w_{11} + b_{11} & \cdots & s'_{1n} \times w_{1n} + b_{1n} \\ \vdots & \ddots & \vdots \\ s'_{l1} \times w_{l1} + b_{l1} & \cdots & s'_{ln} \times w_{ln} + b_{ln} \end{bmatrix} \mathbf{B}_{hm} = \begin{bmatrix} s'_1 \times b'_1 + m'_1 & \cdots & s'_q \times b'_q + m'_q \end{bmatrix}^{\mathrm{T}} \tag{16}$$

The increased migration coefficients are obtained by the PSO algorithm.

The new model obtained by model migration is:

$$Ma_p^{new}(k) = f_o(\mathbf{W}_{hm}^{best}(f_i(\mathbf{W}_{im}^{best} r^{new}(k) - \mathbf{B}_{im}^{best})) - \mathbf{B}_{hm}^{best}) \tag{17}$$

where $\mathbf{W}_{hm}^{best}$, $\mathbf{W}_{im}^{best}$, $\mathbf{B}_{im}^{best}$ and $\mathbf{B}_{hm}^{best}$ are the optimal matrixes of the model transfer coefficients obtained by the PSO algorithm.

The predicted Mach number of the new working condition can be obtained after the output of the prediction model is de-normalized.

In conclusion, the flow chart showing the use of the IOSBC-PSO method to migrate the NARX-BP model of wind tunnel flow field is shown in Figure 3.
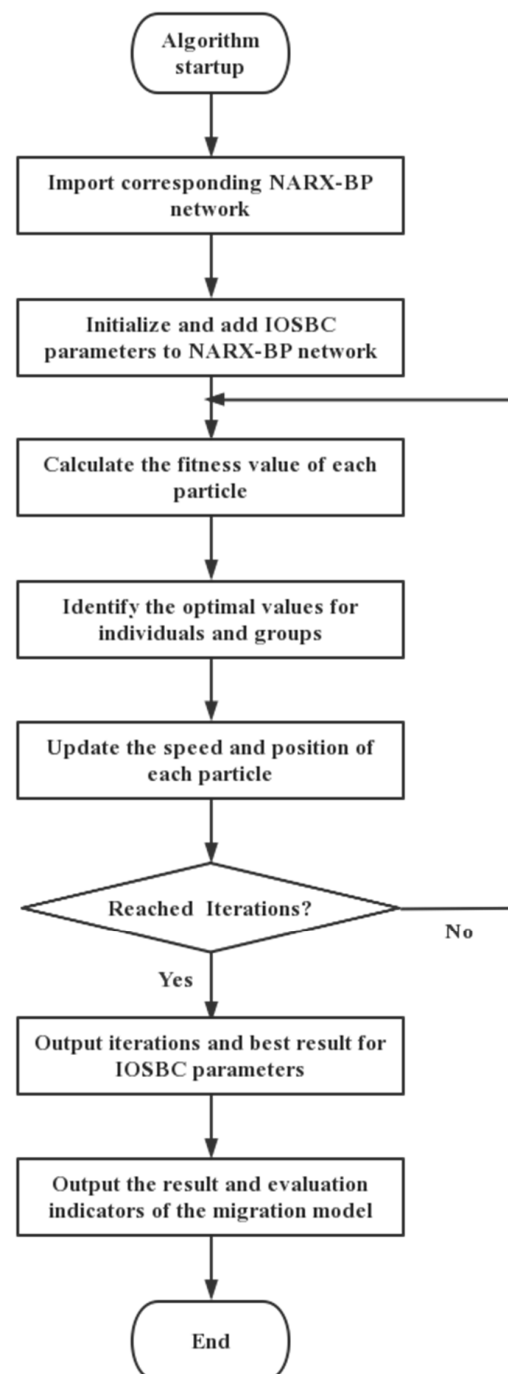
Figure 3. Model migration flow chart based on the IOSBC-PSO method.

3. Illustrative Examples

3.1. Experiment Using the 0.6 m CTWT

Two kinds of working conditions during the operation of a 0.6 m and a 2.4 m CTWT were selected to demonstrate the validity of the established model. First, we had to determine the order of the input variables via the FNN algorithm and then introduce the data into the NARX-BP-based prediction model. Once the prediction results were obtained, evaluation indicators needed to be calculated to evaluate the effectiveness of the proposed model compared with the BP model.

Different working conditions were established in relation to different experimental conditions regarding, e.g., ejector slot, porosity, angle of attack, set Mach number, etc. Different prediction models needed to be built to describe the different working conditions.

Details of data are shown in Table 1.

Table 1. Experimental values chosen for the examined specific working conditions.

Number	Pressure	Ejector Slot	Porosity (%)	Angle of Attack (°)	Set Mach Number	Number of Samples
1	ordinary	24	2	0	0.79	1023
2	ordinary	28	2	0	0.87	670
3	ordinary	28	2.5	0	1.09	1234
4	1.5× boost	28	2	2	0.80	638

Using the FNN algorithm, the order of the variables in the NARX-BP-based prediction model was determined through the analysis for each variable of two typical working conditions shown in Table 1. An efficient FNN computation script written in MATLAB from the University of Potsdam was used [32].

As shown in Figure 4, the FNN simulation results provided the orders that had to be selected for the different variables. For example, the order 3 of Pt corresponded to the inflection point of its percentage decline curve. Based on the FNN theory proposed in Section 2.1, the best order for Pt was 3. Similarly, the best order for Ps, Sp and Ma appeared to be 3, 4, and 3.
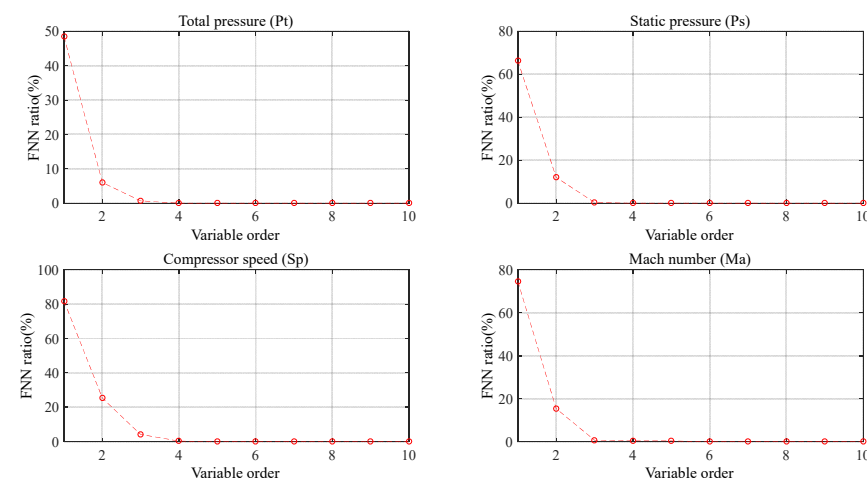
Figure 4. FNN results of working condition 1.

The FNN simulation results of the working conditions 2, 3, 4 and the working condition to be migrated for the 2.4 m CTWT were nearly the same as those for the working condition 1. For the sake of brevity, the simulation results are shown in Table 2. Some variables did not have identical orders and showed fluctuations of 1–2 orders. In this case, the highest variable order was chosen. This approach was based on complete variable information to make the model more precise. In conclusion, the use of the FNN algorithm to determine the

order of *Pt*, *Ps*, *Sp* and *Ma* as 4, 3, 4, 3 can provide complete variable information without redundancy.

Table 2. FNN simulation results of every working condition.

Working Condition	*Pt*	*Ps*	*Sp*	*Ma*
Working condition 1	3	3	4	3
Working condition 2	4	3	4	3
Working condition 3	3	3	3	3
Working condition 4	3	3	4	3
Working condition to be migrated of 2.4 m CTWT	4	3	3	3
Final choice	4	3	4	3

The above conclusion explains why the number of neurons in the input layer of the NARX-BP-based prediction model was chosen as 20. Because the output variable was only the Mach number at the next sampling point, the number of neurons in the output layer was 1. The number of hidden neurons was chosen as 10. The activation functions for the hidden layer and output layer were chosen as sigmoid and linear.

In the NARX-BP-based prediction model, 70% of the data in the two working conditions were selected for neural network training, and the remaining 30% of the data were tested. In most studies without special requirements, for BP neural networks, 70% of the samples are selected as the training set, and 30% of the samples are used as the testing set [33,34]. This choice ensures both a sufficient training sample and the correctness of the test results. The results of the NARX-BP-based prediction model and the BP model as a comparison are shown in Figure 5. The evaluation indicators were calculated and are listed in Table 2.
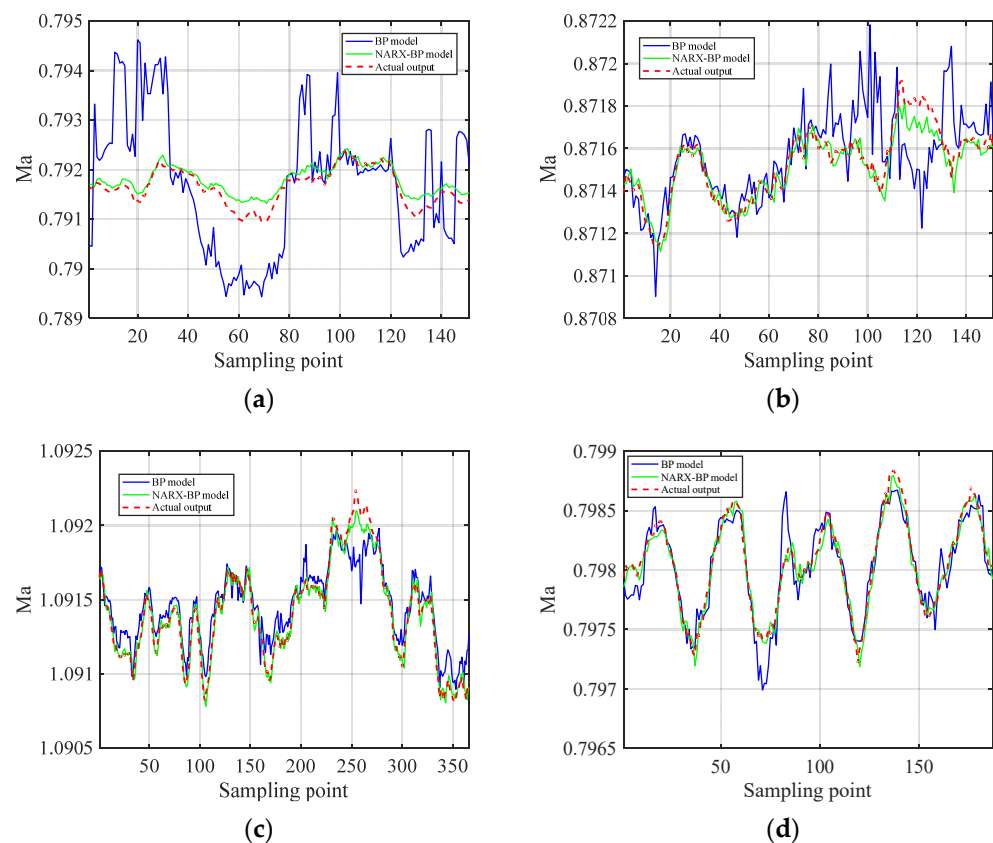
Figure 5. Prediction curves of the Mach number of the NARX-BP model and BP model. (**a**) Working condition 1; (**b**) working condition 2; (**c**) working condition 3; (**d**) working condition 4.

As shown in Figure 5 and Table 3, it could be concluded that in these two working conditions, by introducing the NARX-BP algorithm to build the Mach number prediction model, the model RMSE decreased by 44.93–77.90%, and the MD decreased by 64.05–85.32% compared to the BP model, leading to higher accuracy, higher stability and lower error. The NARX-BP algorithm could meet the error requirements of the project, while the BP network could not. Consequently, the NARX-BP Mach number prediction model is superior to the BP model and can further improve the tracking and prediction ability of the Mach number.

Table 3. Comparison of evaluation indicators in different working conditions.

Working Condition	Algorithm	RMSE/10^{-5}	MD/10^{-4}
Working condition 1	NARX-BP	2.2896	6.5357
	BP	10.3611	32.4258
Working condition 2	NARX-BP	5.6690	1.0170
	BP	17.2910	6.9283
Working condition 3	NARX-BP	5.3112	1.1572
	BP	13.3843	3.2193
Working condition 4	NARX-BP	7.8574	2.2017
	BP	14.2706	5.8804

3.2. Experiment Using the 2.4 m CTWT

Due to the characteristics of the 2.4 m CTWT, in this section, the working condition 1 was chosen as the historical working condition. The data regarding the 2.4 m CTWT are shown in Table 4.

Table 4. Experimental values chosen for the examined specific working conditions of the 2.4 m CTWT.

Wind Tunnel	Pressure	Angle of Attack (°)	Approximate Speed (r·s^{-1})	Set Mach Number	Number of Samples
2.4 m CTWT	ordinary	0	380	0.79	601

It was concluded that the working condition of the new wind tunnel was similar to the working condition 1 from Table 4. Based on that, model migration was feasible.

In order to show the effect of the migration model, only 10% of the new working condition data were selected as the known data, and the remaining data were used as the test data. In order to illustrate the advantages of the migration model, the NARX-BP model and the model based on the IOSBC-GA algorithm were established separately using 10% of the data known in the new working conditions. The Mach number prediction results of the NARX-BP model, IOSBC-GA model and IOSBC-PSO model were compared, as shown in Figures 6 and 7. The parameter settings are listed in Tables 5 and 6.

Table 5. Parameter setting for the PSO algorithm.

Population Size	Iterations	Inertia Weight	Speed Range	Variable Range	Acceleration Factor	Best Fitness
100	200	[0.1, 0.8]	[−0.5, 0.5]	[−1.5, 1.5]	1.5, 2	0.5379

Table 6. Parameter setting for the GA.

Population Size	Iterations	Cross Rate	Mutation Rate	Variable Range	Best Fitness
100	200	0.9	0.1	[−1.5, 1.5]	12.5080
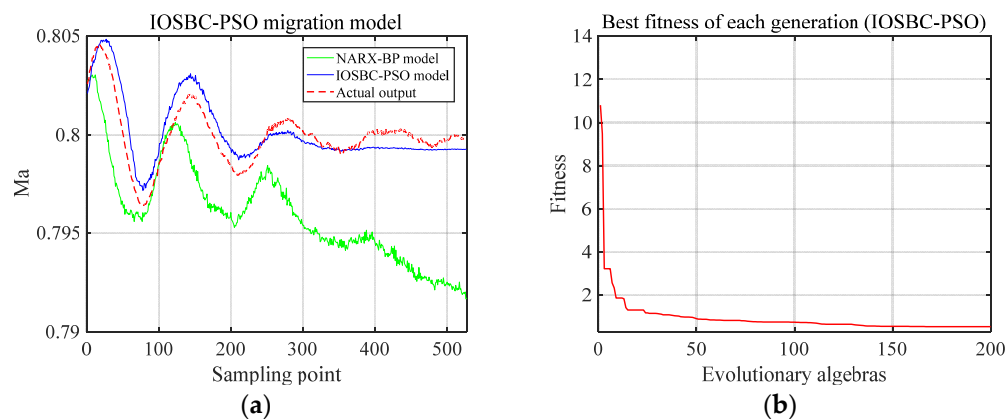
Figure 6. Simulation results using the IOSBC-PSO and NARX-BP models. (**a**) Prediction curves of the Mach number of the NARX-BP model and IOSBC-PSO migration model; (**b**) Fitness curve of the IOSBC-PSO migration model.
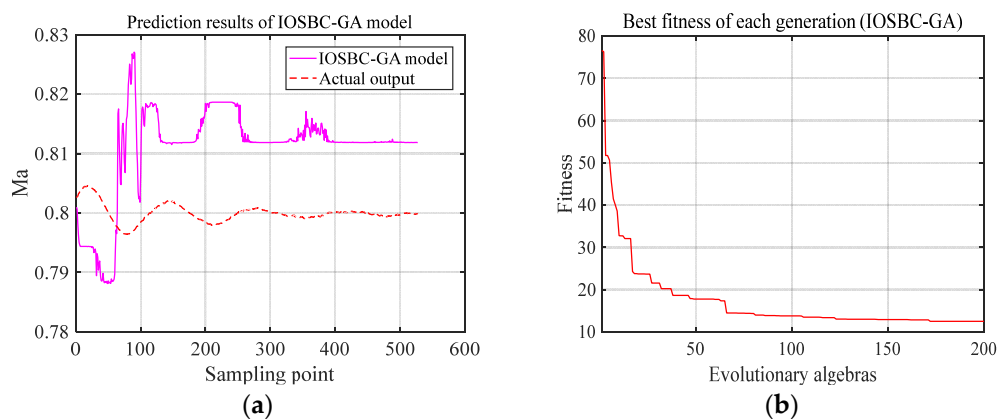
Figure 7. Simulation results using the IOSBC-GA model. (**a**) Prediction curve of the Mach number of the IOSBC-GA migration model; (**b**) Fitness curve of the IOSBC-GA model.

It can be seen in Figures 6a and 7a that the Mach number predicted by the IOSBC-PSO model was closer to the actual Mach number than those predicted by the IOSBC-GA model and the NARX-BP model. According to Figures 6b and 7b, the fitness convergence of the PSO model was better than that of the GA model, indicating that the prediction ability of the PSO model was better.

The evaluation indicators of the three models were calculated for comparison and are displayed in Table 7.

Table 7. Comparison of the evaluation indicators of the three algorithms.

Algorithms	Simulation Time/s	RMSE/10^{-5}	MD/10^{-4}
IOSBC-PSO	581.34	8.1238	4.6893
IOSBC-GA	1478.38	140.6351	300.7827
NARX-BP	1.6772	45.2948	21.5627

In shown in Table 7, as a non-migration model, the NARX-BP model did not need iterative processing to calculate its parameters; so, it required little calculation time. However, the performance of the IOSBC-PSO model, as shown by the RMSE and MD indicators, was far better than those of the other two algorithms, and the calculation time of the IOSBC-PSO model migration was far shorter than those of the other migration algorithms. The IOSBC-PSO algorithm could meet all the requirements in the determination of the evaluation

indicators, while the remaining two algorithms could not. The model RMSE decreased by 82.06%, and the MD decreased by 78.25% compared to those of the non-migration model. Therefore, the conclusion can be drawn that the proposed method is effective in solving the model migration problem. The proposed method achieved error tolerance in the project; so, the IOSBC-PSO migration algorithm can be used to model a new working condition with just an old model and a small amount of data, without spending much manpower and resources on wind tunnel blowing experiments, which is of great significance to the wind tunnel test research.

4. Conclusions

The modeling strategy for the Mach number prediction model of a 0.6 m CTWT with sufficient experimental data and the migration model of a 2.4 m CTWT with less experimental data was investigated. Compared with the BP model, the FNN-NARX-BP approach met all the requirements in the determination of the evaluation indicators and significantly outperformed the BP model in terms of model stability and accuracy. For model migration, the IOSBC-PSO approach was proposed and outperformed both the IOSBC-GA approach and the non-migration model in terms of RMSE and MD. The superiority of the proposed method was clearly illustrated. The method proposed in this paper has certain practical significance due to the fact that once the prediction model of the Mach number of the wind tunnel is established, the predictive controller of the Mach number can be designed to control the wind tunnel in a practical situation.

However, only a Mach number prediction model based on the NARX-BP algorithm and a migration model based on the IOSBC-PSO algorithm were proposed in this paper. Further study of the Mach number control strategy in the prediction model is necessary to increase the practical application value of the Mach number prediction model.

Author Contributions: Conceptualization, L.Z.; methodology, L.Z., Y.S. and W.J.; software, W.J.; validation, Y.S. and W.J.; formal analysis, W.J.; investigation, L.Z.; resources, L.Z.; data curation, L.Z.; writing—original draft preparation, Y.S. and W.J.; writing—review and editing, L.Z.; visualization, Y.S. and W.J.; supervision, L.Z.; project administration, L.Z.; funding acquisition, L.Z. All authors have read and agreed to the published version of the manuscript.

Data Availability Statement: Not applicable.

Conflicts of Interest: The authors declare no conflict of interest.

References

1. Yang, G.T.; Tang, S.J.; Guo, J. *Aerodynamic Optimization of a Morphing UAV with Variable Sweep and Variable Span, CSSE2014 ed.*; WIT Press: Billerica, MA, USA, 2014; pp. 570–578.
2. Wang, Y.G.; Jian, S.T.; Wang, Z.G.; Fan, R.; Han, P.; Lyu, Y. An Intelligent Algorithm for Aerodynamic Parameters Calibration of Wind Tunnel Experiment at a High Angle of Attack. *Int. J. Aerosp. Eng.* **2023**, *2023*, 3093526. [CrossRef]
3. Chen, C.; Klaus, T. Wind tunnel tests on the unsteady galloping of a bridge deck with open cross section in turbulent flow. *J. Wind Eng. Ind. Aerodyn.* **2023**, *233*, 105293. [CrossRef]
4. Huang, B.; Li, Z.; Gong, B.; Zhang, Z.; Shan, B.; Pu, O. Study on the sandstorm load of low-rise buildings via wind tunnel testing. *J. Build. Eng.* **2023**, *65*, 205821. [CrossRef]
5. Esteban, A.R.C.; Elia, B.; Gisella, T. Evaluation of the aerodynamic effect of a smooth rounded roof on crosswind stability of a train by wind tunnel tests. *Appl. Sci.* **2023**, *13*, 232.
6. Yang, X.; Wang, X.Y.; Zhu, J.H.; Yan, W. Modelling, analysis and experimental study of the prop-rotor of vertical/short-take-off and landing aircraft. *Proc. Inst. Mech. Eng. Part G J. Aerosp. Eng.* **2022**, *236*, 2851–2884. [CrossRef]
7. Zhang, L.; Ma, D.; Yang, M.; Yao, Y.; Yu, Y.; Yang, X. Experimental and numerical study on the performance of double membrane wing for long-endurance low-speed aircraft. *Appl. Sci.* **2022**, *12*, 6765. [CrossRef]
8. Jarugumilli, T.; Benedict, M.; Chopra, I. Wind tunnel studies on a micro air vehicle-scale cycloidal rotor. *J. Am. Helicopter Soc.* **2014**, *59*, 1–10. [CrossRef]
9. Wang, Q.; Luo, K.; Wu, C.; Tan, J.; He, R.; Ye, S.; Fan, J. Inter-farm cluster interaction of the operational and planned offshore wind power base. *J. Clean. Prod.* **2023**, *396*, 136529. [CrossRef]

10. Wang, Q.; Luo, K.; Wu, C.; Fan, J. Impact of substantial wind farms on the local and regional atmospheric boundary layer: Case study of Zhangbei wind power base in China. *Energy* **2019**, *183*, 1136–1149. [CrossRef]

11. Wang, Y.; Wang, Z.G.; Liang, J.H.; Fan, X. Investigation on hypersonic inlet starting process in continuous free jet wind tunnel. *J. Propuls. Power* **2014**, *30*, 1721. [CrossRef]

12. Aboelezz, A. Low speed wind tunnel design and optimization using computational techniques and experimental validation. *INCAS Bull.* **2019**, *11*, 3–13. [CrossRef]

13. Wu, J.; Radespiel, R. Tandem nozzle supersonic wind tunnel design. *Int. J. Eng. Syst. Model. Simul.* **2013**, *5*, 8–18. [CrossRef]

14. Piccirillo, P.; Atta, C.W. A multiple-source wind tunnel design for producing turbulent shear flows in a stably stratified fluid. *Exp. Fluids* **1996**, *21*, 66–69. [CrossRef]

15. Zhao, Z.; Zhao, Z.W.; Yan, Y.; Zeng, K.; Shi, X.; Wu, H. Dynamics, stability, and control of a four-cable mount system for wind tunnel test. *Chin. J. Aeronaut.* **2023**, *36*, 58–75. [CrossRef]

16. Li, J.; Wang, H.; Huang, H.L. Application of high-speed wind tunnel control based on PID neural network. *Adv. Eng. Forum.* **2011**, *2–3*, 3–6. [CrossRef]

17. Andrei, N.C. Blowdown wind tunnel control using an adaptive fuzzy PI controller. *INCAS Bull.* **2013**, *5*, 89–98. [CrossRef]

18. Guo, J.; Zhang, R.; Cui, X.; Tianle, H.; Xin, H.; Zhao, L. Model transfer and fuzzy PID control of Mach number of wind tunnel flow field. In Proceedings of the 2020 Chinese Automation Congress (CAC), Shanghai, China, 6–8 November 2020; pp. 6923–6927.

19. Lu, J.D.; Yao, K.; Gao, F.R. Process similarity and developing new process models through migration. *AIChE J.* **2009**, *55*, 2318–2328. [CrossRef]

20. Tang, X.P.; Gao, F.R.; Lai, X. Compressing and reconstructing the voltage data for lithium-ion batteries using model migration and un-equidistant sampling techniques. *eTransportation* **2022**, *13*, 100186. [CrossRef]

21. Lu, J.; Gao, F. Process modeling based on process similarity. *Ind. Eng. Chem. Res.* **2008**, *47*, 1967–1974. [CrossRef]

22. Tao, C.; Yang, O. Modeling of scramjet combustors based on model migration and process similarity. *Energies* **2019**, *12*, 2516.

23. Broomhead, D.S.; King, G.P. Extracting qualitative dynamics from experimental data. *Phys. D Nonlinear Phenom.* **1986**, *20*, 217–236. [CrossRef]

24. Kennel, M.B.; Brown, R.; Abarbanel, H.D. Determining embedding dimension for phase-space reconstruction using a geometrical construction. *Phys. Rev. A* **1992**, *45*, 3403–3411. [CrossRef] [PubMed]

25. Aksamit, N.O.; Whitfield, P.H. Examining the pluvial to nival river regime spectrum using nonlinear methods: Minimum delay embedding dimension. *J. Hydrol.* **2019**, *572*, 851–868. [CrossRef]

26. Leontaritis, I.J.; Billings, S.A. Input-output parametric models for non-linear systems Part I: Deterministic non-linear systems. *Int. J. Control* **1985**, *41*, 303–328. [CrossRef]

27. Hadi, M.; Sajjad, M.; Leili, F.; Sabaei, M. PSO-ELPM: PSO with elite learning, enhanced parameter updating, and exponential mutation operator. *Inf. Sci.* **2023**, *628*, 70–91.

28. Rumelhart, D.; Hinton, G. Learning representations by back-propagating errors. *Nature* **1986**, *323*, 533–536. [CrossRef]

29. Kennedy, J.; Eberhart, R. Particle swarm optimization. In Proceedings of the ICNN'95—International Conference on Neural Networks, Perth, WA, Australia, 27 November–1 December 1995; Volume 4, pp. 1942–1948.

30. Shi, Y.; Eberhart, R. A modified particle swarm optimizer. In Proceedings of the IEEE World Congress on Computational Intelligence, Anchorage, AK, USA, 4–9 May 1998; pp. 69–73.

31. Hassan, R.; Cohanim, B.; de Weck, O.; Venter, G. A comparison of particle swarm optimization and the genetic algorithm. In Proceedings of the 46th AIAA/ASME/ASCE/AHS/ASC Structures, Structural Dynamics and Materials Conference, Austin, TX, USA, 18–21 April 2005.

32. Marwan, N. Cross Recurrence Plot Toolbox 5.24 (R34) [Internet]. 2022. Available online: https://tocsy.pik-potsdam.de/CRPtoolbox/?q=content_install (accessed on 10 March 2023).

33. Zhang, Y.; Wang, Y.J.; Zhang, Y.; Yu, T. Photovoltaic fuzzy logical control MPPT based on adaptive genetic simulated annealing algorithm-optimized BP neural network. *Processes* **2022**, *10*, 1411. [CrossRef]

34. Li, Q.W.; Jia, W.C. Phase selection and location method of generator stator winding ground fault based on BP neural network. *Energies* **2023**, *16*, 1503. [CrossRef]